


## FULL ARTICLE

# Race-specific differences in the phase coherence between blood flow and oxygenation: A simultaneous NIRS, white light spectroscopy and LDF study

Yunus A. Abdulhameed<sup>1,2</sup> | Peter V. E. McClintock<sup>1</sup> | Aneta Stefanovska<sup>1\*</sup> <sup>1</sup>Department of Physics, Lancaster University, Lancaster, UK<sup>2</sup>Department of Physics, Yusuf Maitama Sule University, Kano, Nigeria**\*Correspondence**

Aneta Stefanovska, Department of Physics, Lancaster University, Lancaster, UK.

Email: aneta@lancaster.ac.uk

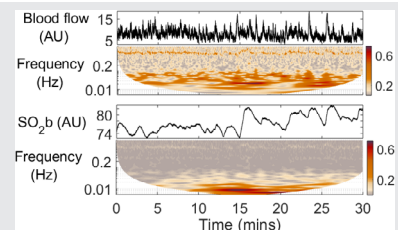
**Funding information**

Engineering and Physical Sciences Research Council, Grant/Award Number: EP/M006298/1; Javna Agencija za Raziskovalno Dejavnost RS; Joy Welch Educational Charitable Trust (UK); Petroleum Technology Development Fund (Nigeria), Grant/Award Number: PTDF/ED/OSS/PHD/1120/17; Tertiary Education Trust Fund (Nigeria)

**Abstract**

Race-specific differences in the level of glycated hemoglobin are well known. However, these differences were detected by invasive measurement of mean oxygenation, and their understanding

remains far from complete. Given that oxygen is delivered to the cells by hemoglobin through the cardiovascular system, a possible approach is to investigate the phase coherence between blood flow and oxygen transportation. Here we introduce a noninvasive optical method based on simultaneous recordings using NIRS, white light spectroscopy and LDF, combined with wavelet-based phase coherence analysis. Signals were recorded simultaneously for individuals in two groups of healthy subjects, 16 from Sub-Saharan Africa (BA group) and 16 Europeans (CA group). It was found that the power of myogenic oscillations in oxygenated and de-oxygenated hemoglobin is higher in the BA group, but that the phase coherence between blood flow and oxygen saturation, or blood flow and hemoglobin concentrations is higher in the CA group

**KEYWORDS**

blood flow, ethnic, laser Doppler flowmetry, near-infrared spectroscopy, oxygenation, physiological oscillations, wavelet phase coherence, white light spectroscopy

## 1 | INTRODUCTION

There are known differences in cardiovascular dynamics between people of Sub-Saharan African descent and European descent [1–3]. They manifest both clinically, as in the prevalence of diabetes and other vascular diseases [4], and also in terms of differences in vasodilation and vasoconstriction processes [1, 5–9]. The latter differences could perhaps be related to variations in gene expression between the races. Studies of these differences can

further illuminate race-related distinctions in cardiovascular function, which are known to be influenced by gene expression, whence the different susceptibilities to certain diseases [4, 10]. Vasodilation and vasoconstriction have close relationships with the delivery and regulation of blood, serving to ensure the proper oxygen supply. Endothelium-dependent vasodilation and endothelium-dependent vasoconstriction are of wide-ranging importance for protecting the microvascular system against pathophysiological insults [11, 12].

This is an open access article under the terms of the Creative Commons Attribution License, which permits use, distribution and reproduction in any medium, provided the original work is properly cited.

© 2020 The Authors. *Journal of Biophotonics* published by WILEY-VCH Verlag GmbH & Co. KGaA, Weinheim

To the best of our knowledge, no previous study of race-related differences in blood flow and tissue oxygenation dynamics (BFOD) has been published, so that race-specific differences at the level of microvascular blood flow and tissue oxygenation are still unknown. Earlier studies investigated ethnic differences in the oscillations that manifest in heart rate variability (HRV), using Fourier transformation [13]. But this approach is incapable of tracing either the time evolution of high frequency oscillations or low frequency events in a nonsinusoidal [13–15] signal such as HRV and, even if properly revealed, their mutual interaction and even causal mechanism remains unknown. The identification of rhythmic mutual coordination between two distinct oscillators requires at least the detection of their 1:1 synchronization. Wavelet coherence [16] was introduced to study such synchronization. Later, wavelet phase coherence was introduced [17, 18] which detects whether or not the difference in phase between two signals at a given frequency remains constant in time. In contrast to spectral power, phase coherence has been shown to be relatively free of noise effects and to allow the detection of coordination between two distinct signals [17].

To try to reach an understanding of the differences in microvascular blood flow and tissue oxygenation between people of Sub-Saharan Africans and Europeans, the present study exploits two specific advances; (a) a novel system that enables simultaneous monitoring of blood flow and oxygenation in the same area and (b) recently developed methods based on wavelet phase coherence to establish, not only the intensity of various oscillatory process involved in cardiovascular regulation, but also their degree of coordination.

Blood flow dynamics [11, 19, 20], oxygen saturation and hemoglobin concentration all comprise fluctuations around central, but time-varying, values [21–24]. The extent to which hemoglobin binds oxygen determines the amount of oxygen transported around the body, its organs and cells. Oxygen-hemoglobin fluctuations alongside oxygen circulation have been extensively explored, and date back to the work of August Krogh in 1919, who pioneered the *in vitro* study of oxygen transport [25, 26]. He measured not only the diffusion coefficients for oxygen in different tissues, but also the average distances traveled by oxygen molecules from a capillary to the site of chemical reaction. This work inspired several other investigations into blood oxygenation fluctuations, leading to new insights into oxygenation dynamics in both the healthy and pathological states [24, 27–31].

Investigations based on continuous glucose monitoring in diabetic patients have also demonstrated race-specific differences in the level of glycated hemoglobin (HbA<sub>1c</sub>) for a given mean glucose concentration, with the glycation gap being attributed to genetic difference

[32, 33]. Reports of such HbA<sub>1c</sub> differences are well-documented for both type 1 and type 2 diabetes, with non-Hispanic subjects having lower HbA<sub>1c</sub> levels than blacks [33–39]. The raised HbA<sub>1c</sub> level in blacks has been attributed to poor glycemic control [40].

Despite the inconvenience of obtaining HbA<sub>1c</sub> invasively, its mean value has been used widely in studying the corresponding race-specific differences. In fact, understanding of the role of the race-related disparity in HbA<sub>1c</sub> is still far from complete because mean oxygenation is not a sufficient measure of the physiological situation [28]. Given that oxygen is delivered to the cells by hemoglobin (Hb) through the cardiovascular system, a possible route to a deeper understanding of the race-related differences in HbA<sub>1c</sub> is to investigate the oscillatory fluctuations in blood flow and oxygen transportation.

A noninvasive system for monitoring oxygenation fluctuations is potentially helpful for investigating race-related differences within a continuous time frame. Near-infrared spectroscopy (NIRS) [41, 42], white light spectroscopy [43, 44] and laser Doppler flowmetry (LDF) [45, 46] can contribute to such a system. They are all continuous optical methods that allow for real-time monitoring of changes in both the systemic and local activities of the cardiovascular system. Systemic activities, reflecting the heart function and respiration alongside local activities modulated by vasomotion, might affect tissue oxygenation [23, 47–49].

Earlier studies have not only investigated the oscillations in NIRS oxygenation [50], but have also used optical reflectance spectroscopy (which is a form of NIRS) to determine the coherence between fluctuations in BFOD using wavelet-based analysis [30]. They demonstrated coherence between LDF blood flow and oxygenation in the skin microcirculation [30]. However, NIRS devices used in recent studies of tissue oxygenation have mostly been used to evaluate oxygen saturation at the capillary level [47, 51–53]. This can only reveal local information about oxygen utilization. The development of a combined white light reflectance and LDF probe that uses a single-point low-power infrared light source (785 nm) and white light (400–700 nm) excitation, respectively, has enabled simultaneous recordings of blood flow and oxygenation at the same location [43, 44]. This can illuminate their mutual interactions to provide more information about oxygenation mechanisms in the microcirculation.

LDF allows one to observe the systemic and local physiological processes of microvascular blood flow *in vivo* in both lightly and darkly pigmented skin [54]. Furthermore, LDF has the ability to record blood flow continuously with high temporal resolution and can provide information on microvascular control processes [19]. These features can help us to further investigate the effect of racial differences in the six distinct oscillatory

processes of microvascular dynamics [11, 19, 20, 55, 56]. These span an interval of 0.0095 to 2 Hz: interval I (0.6-2 Hz) is related to cardiac activity; interval II (0.145-0.6 Hz) is related to respiratory activity; interval III (0.052-0.145 Hz) is related to microvessel smooth muscle cell activity; interval IV (0.021-0.052 Hz) is related to microvessel innervation; and intervals V and VI (0.0095-0.021 and 0.005-0.0095 Hz, respectively) are related to endothelial activity, and are respectively nitric oxide (NO) dependent and independent.

It is against this background that the present study used a novel system combining LDF at 785 nm with a single infra-red light source for NIRS at 750 nm and 850 nm, and a 400 to 700 nm white light source to investigate race-specific differences in coherence between the fluctuations in blood flow and oxygenation dynamics. The presence of oscillations was checked from the signals using wavelet analysis. Wavelet phase coherence was used to investigate the interactions between simultaneously recorded pairs of signals; (a) the microvascular LDF blood flow and NIRS oxygenation from the deep skin (OXY: oxyHb, deoxyHb,  $SO_2\%$ ) signals and (b) the microvascular LDF blood flow and white light oxygenation from the superficial skin (OXY: oxyHb, deoxyHb,  $SO_2\%$  (where  $SO_2$  means saturated oxygen).

## 2 | METHODS

### 2.1 | Participants

The 32 volunteers participating in the study were all male adults, with age ranges as given in Table 1. They were divided into two groups: 16 black Africans (BA) and 16 Caucasian whites (CA), all students at Lancaster University. The BA group was composed of West Africans (from Nigeria and Ghana) plus two black Sudanese, while the CA group was white-skinned British plus two Europeans. All volunteers were nonsmokers, and not taking any medications. They were asked to refrain from taking caffeine or food for at least 2 hours prior to the measurements. Subjects were allowed at least 20 minutes to become acclimatized to room temperature. They were requested to refrain from body movements as far as possible while measurements were in progress. During the 30 minutes of recording, subjects lay relaxed in a supine

state, in a temperature controlled room ( $20 \pm 2^\circ\text{C}$ ). General data for the two groups are summarized in Table 1 including their body mass indices (BMI). Individuals in the CA group had lived their lives in the UK at an altitude not higher than 50 m above sea level and with an average annual temperature of  $10^\circ\text{C}$ , except for two persons from Belarus and Turkey, respectively. Individuals in the BA group had lived for more than 80% of their lives at an average altitude of 470 m and with an average annual temperature of  $26.8^\circ\text{C}$  (see Table 2). All subjects had normal blood pressure, with systolic blood pressure (SBP)  $< 140$  mm Hg and diastolic BP  $< 90$  mm Hg. All had heart rate  $< 1.2$  Hz, BMI  $< 24.9$  and skin temperature (ST)  $< 29^\circ\text{C}$ . Participants gave their informed consent and the study was approved by the Faculty of Science and Technology Research Ethics Committee, of Lancaster University, UK.

### 2.2 | Acquisition of microvascular blood flow and oxygenation signals

The microvascular blood flow and oxygenation dynamics were quantified by use of: (a) a moorVMS-LDF2 laser Doppler flowmetry instrument to measure blood flow; (b) a moorVMS-OXY white light reflectance spectroscopy monitor to measure oxygenation; and (c) a moorVMS-NIRS near-infra-red spectrometer to measure oxygenation at a deeper level in the tissue than (b). Sensors from (a) and (b) were integrated into the same physical unit. All were manufactured by Moor Instruments Ltd, Axminster, UK. Each signal (Figure 1) was recorded on the left ventral forearm for 30 minutes at a sampling frequency of 40 Hz. The group median values and ranges of blood flow, oxygen saturation and hemoglobin concentration are presented in Table 3. We now summarize the working principles of the individual instruments.

#### 2.2.1 | Microvascular blood flow

##### *moorVMS-LDF2 laser Doppler flowmetry*

The LDF instrument incorporates a temperature-stabilized laser diode generating infrared laser light of wavelength 785 nm at an output power of 2.5 mW. The light is transmitted via a flexible optical fiber to a sensor

**TABLE 1** Anthropometric data of measured subjects, median values and ranges (25th percentile and 75th percentile)

Group	Age (y)	BMI ( $\text{kg}/\text{m}^2$ )	ST ( $^\circ\text{C}$ )	Heart rate (Hz)	SBP (mm Hg)	DBP (mm Hg)
BA	26.5 [20.5 33.0]	21.2 [18.1 24.1]	29.7 [28.3 30.7]	0.99 [0.97 1.14]	116 and 133 [116 133]	76.5 [71.5 81.0]
CA	22.5 [19.0 26.0]	23.1 [21.0 24.8]	29.8 [28.8 30.4]	0.96 [0.83 1.08]	123 [109 127]	77.0 [68.0 80.0]

Abbreviations: BMI, body mass index; DSP, diastolic blood pressure; SBP, systolic blood pressure; ST for skin temperature.

**TABLE 2** Information about the country, altitude, and temperature of the sub-Saharan participants recruited for the study

Subject	Altitude (m)	State/Country	Annual mean temperature (°C)
1	381	Sudan	29.9
2	381	Sudan	29.9
3	1053	Ondo/Nigeria	25.3
4	519	Katsina/ Nigeria	26.4
5	200	Benin/Nigeria	26.1
6	250	Kaduna/ Nigeria	25.2
7	41	Lagos/Nigeria	27.1
8	450	Abuja/Nigeria	25.7
9	41	Lagos/Nigeria	27.1
10	299	Yobe/Nigeria	25.2
11	41	Lagos/Nigeria	27.1
12	488	Kano/Nigeria	26.4
13	488	Kano/Nigeria	26.4
14	2359	Niger/Nigeria	27.5
15	41	Lagos/Nigeria	27.1
16	488	Kano/Nigeria	26.4

Note: Note that each participant had lived more than 80% of his life in the country.

accommodated in a flexible probe-holder, held in place on the skin with a double sided adhesive disk. After passing through the skin and reaching the microvasculature, light is scattered by red blood cells. Because the latter are moving the back-scattered light is frequency-shifted by the Doppler effect; it is then returned to the instrument via a second optical fiber. The frequency difference between the incident and back-scattered light yields the LDF signal, known as the blood perfusion signal. The blood flow signal obtained is expressed in perfusion units (PU) of output voltage (typically 100 PU = 5 V).

### 2.2.2 | Tissue oxygenation

The oxygenation level in tissue is determined by a balance between oxygen delivery and oxygen utilization. Oxygen saturation is not a direct measure of tissue oxygenation, as several physiological factors such as tissue pH and temperature, influence the affinity of oxygen for hemoglobin, which determines the adequacy of oxygen supply to the tissues.

### *moorVMS-NIRS and moorVMS-OXY*

The moorVMS-NIRS and moorVMS-OXY modules were both used for measurement of oxygenation (oxygen saturation, oxygenated and deoxygenated hemoglobin concentrations). The moorVMS-NIRS determined oxygen saturation in deeper tissue layers, using the traditional spatially resolved spectroscopy method [57, 58] to calculate the absolute concentrations of oxygenated hemoglobin (oxyHb) and deoxygenated hemoglobin (deoxyHb) in tissue. The moorVMS-OXY system measures the oxygenation (oxygen saturation, oxygenated and deoxygenated hemoglobin concentrations) in more superficial tissue layers.

Both instruments functioned in a similar manner, using emitter and detector probes placed on the left ventral forearm. For the moorVMS-NIRS, two near infrared LEDs emitted light with peak wavelengths of 750 and 850 nm with spectral distributions of 60 and 80 nm, respectively, and maximum output power of 12 mW at each wavelength; for the moorVMS-OXY, a Moor CP7-1000 blunt needle probe is placed in contact with the skin, consisting of a photodiode generating white light over the wavelength range 400 to 700 nm with a maximum optical output power of 6 mW. In each case, a small proportion of the light from the emitter penetrates through the tissue and is reflected back from (mostly) erythrocytes, to reach the photodiodes.

In the moorVMS-NIRS, there are two identical detector photodiodes placed 0.5 cm apart. Based on their relative orientation, the oxygen-dependent absorption characteristics exhibited by tissue chromophores (hemoglobin) in the region under investigation is obtained by evaluating the relationship between the light attenuation and tissue chromophore concentration using the modified Beer-Lambert law [57], that is, assuming linearity of attenuation with chromophore concentration. Thus the dynamical change in hemoglobin concentration can be found. The orientation of the photodetectors allows the variation in the attenuation to be measured [28].

The attenuation coefficient of tissue is obtained by computing the spatial variation of the retro-reflected light intensity as a function of distance between the light emitted at high source-to-detector spacings [59]. Using the known optical characteristics of hemoglobin, known probe geometry, and postulates about typical tissue scattering characteristics, the absolute concentrations of oxyHb and deoxyHb can then be calculated. The back-scattered light collected through the photodiode is received at the detector and amplified. The signals were recorded using MoorSoft software. Data were exported to Matlab (R2016b, Mathworks, UK) for preprocessing and analysis.

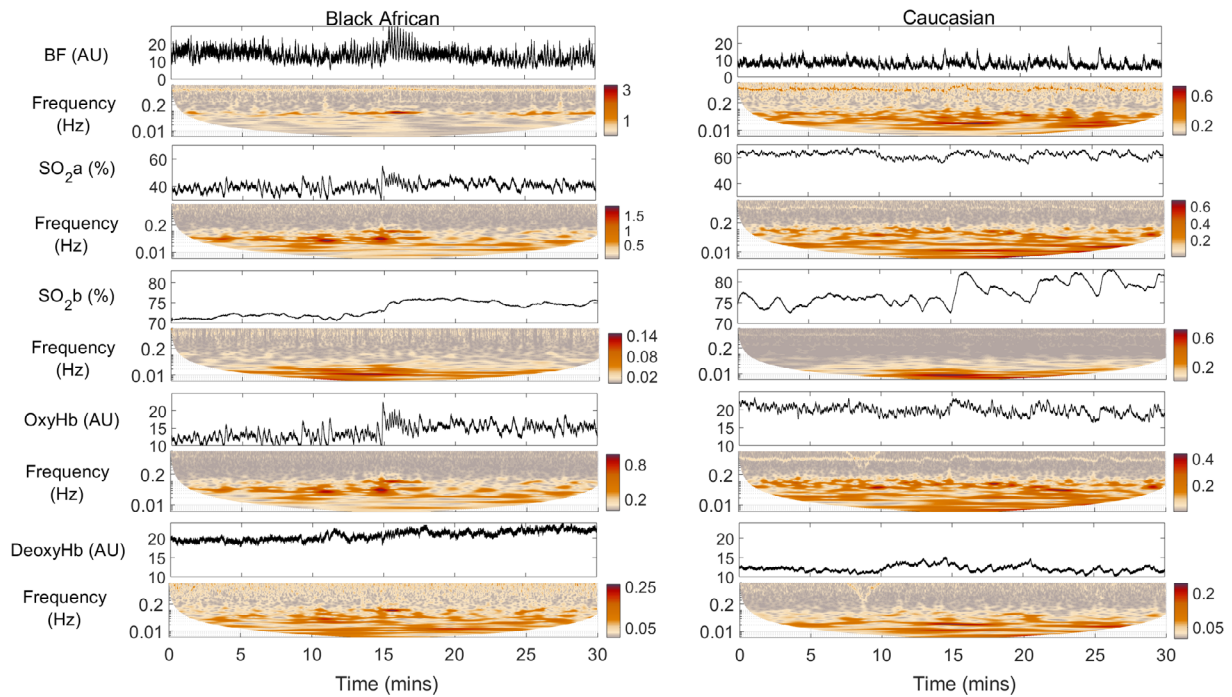


**FIGURE 1** Simultaneous recordings of blood flow (BF) using LDF, oxygen saturation  $SO_{2a}$  using white light spectroscopy, oxygen saturation  $SO_{2b}$  using NIRS, oxygenated hemoglobin (oxyHb) and deoxygenated hemoglobin (deoxyHb) using white light spectroscopy with their respective continuous wavelet representations (below each time-series) for a typical black African from the BA group, and a typical Caucasian (CA group). For each subject, signals were simultaneously recorded from the skin of the left ventral forearm, for 30 minutes. The wavelet transform enables accurate visualization of the frequency content of the time-series over time

**TABLE 3** Median values and ranges (25th percentile and 75th percentile) of blood flow, oxygen saturation ( $SO_{2a}$ , measured at a shallow depth in the skin using white light spectroscopy,  $SO_{2b}$ —measured deeper in the skin using NIRS), oxygenated, and deoxygenated hemoglobin concentrations

Signal	BA	CA	P value
Blood flow (AU)	9.3 [7.9 15.2]	13.7 [8.1 19.8]	.23
Oxygen saturation, $SO_{2a}$ (%)	35.4 [29.2 39.6]	48.6 [39.6 59.4]	.002
Oxygen saturation, $SO_{2b}$ (%)	65.2 [59.9 68.4]	68.1 [66.5 71.6]	.03
Oxygenated hemoglobin (AU)	14.5 [12.9 17.0]	7.4 [5.9 12.0]	.002
Deoxygenated hemoglobin (AU)	29.0 [24.6 31.9]	8.3 [7.3 12.2]	.0000001

The moorVMS-OXY system is based on the established theory of white light reflectance spectroscopy. The oxygenation signal obtained with VMS-OXY system is premised on spectrophotometric principles that relate light absorption to chromophore concentrations. Some light is absorbed by the erythrocytes, depending on the wavelength and on their Hb oxygenation status. A fraction of the light is reflected, and

returned by another optical fiber in the same probe; some portion of the light is absorbed by the hemoglobin. The fraction absorbed depends on two parameters: the light's wavelength and the level of oxygenation. The color of the tissue, which provides the basis of the spectroscopic measurements used by the moorVMS-OXY system [60], is determined by both the hemoglobin concentration in the tissue and the oxygen saturation. Similarly to the case of NIRS (see above), the system then computes tissue oxygenation by comparing the collected spectra with the absorption curves from known concentrations of oxyHb and deoxyHb. Skin temperature was also recorded via a thermistor incorporated in probe tip. The output tissue oxygenations  $SO_{2a}$  and  $SO_{2b}$ , measured with VMS-OXY and VMS-NIRS, respectively, are expressed in % of output voltage (typically, 100% = 5 V for  $SO_{2a}$  and 100% = 1 V for  $SO_{2a}$ ). Mathematically,  $SO_2$  (%) is generally defined as

$$SO_2 = \frac{\text{oxyHb}}{\text{totalHb}} \times 100\%, \quad (1)$$

where total hemoglobin (totalHb) = oxygenated hemoglobin (oxyHb) + deoxygenated hemoglobin (deoxyHb). Each of the hemoglobins is measured in arbitrary units (AU).

## 2.3 | Signal analysis

### 2.3.1 | Wavelet transform

The spectral content of the recorded signals was established by application of the continuous wavelet transform (WT). The WT is more suitable than the windowed Fourier transform for nonstationary signals like those in the present study, partly because it can have logarithmic frequency resolution. It uses a full range of wavelet scales at each location, and can be tuned, depending on the frequency ranges we wish to investigate. The WT is a scale-independent method comprising an adaptive window-length allowing low frequencies to be analyzed using long wavelets and higher frequencies with short wavelets. The continuous WT  $W_s(s, t)$  of a signal  $f(t)$  is defined as

$$W_s(s, t) = |s|^{-1/2} \int_{-\infty}^{\infty} \psi\left(\frac{u-t}{s}\right) f(u) du. \quad (2)$$

where  $s$  is the scaling factor,  $t$  is the temporal position on the signal and the wavelet function is built by scaling and translating a chosen mother wavelet  $\psi$  which, in this study, is chosen to be the complex Morlet wavelet (Equation 3) because it maximizes joint time-localisation and frequency-resolution [19].

$$\psi(u) = \frac{1}{\sqrt{\pi}} \left( e^{-i\omega_0 u} - e^{-\omega_0^2/2} \right) e^{-u^2/2}. \quad (3)$$

Note that the variable  $u$  is real number that allows a trade-off between the time-localisation and frequency-resolution. There is a direct inverse relationship between the scaling factor  $s$  and its corresponding frequency,  $f = 1/s$ .

### 2.3.2 | Wavelet phase coherence

While waves can be coherent in space, oscillations are known to be coherent in time. Quite generally, correlation properties between physical quantities, whether at a single or several oscillation frequencies, can be studied by investigating their coherence in time. If we observe oscillations at the same frequency in two different time series and find that the difference between their instantaneous phases  $\phi_{1k,n}$  and  $\phi_{2k,n}$  is constant, then the oscillations are said to be coherent at that frequency [17, 18, 30]. A phenomenon closely related to coherence is that of phase synchronization [61–64]. While oscillations can be coherent without necessarily being directly coupled, the existence of coupling is fundamental for synchronization [65]. For example, if we have an  $n:m$  relationship between the frequencies of two signals (eg, blood flow and oxygen saturation), this implies that there are

$n$  oscillation cycles in one time series per  $m$  cycles of the other time series: 1:1 phase synchronization may equally be considered as phase coherent oscillations. Thus phase coherence can be used directly to investigate 1:1 synchronization between two signals, such as the blood flow and oxygen saturation signals used in the present study. The wavelet phase coherence (WPC)  $\gamma(f)$  between the two signals  $f_1(t)$  and  $f_2(t)$  is estimated through their respective WTs as obtained in Equation (2), that is,  $W_{s_{1,2}}(t, f)$  [19] as

$$\gamma(f) = \left| \frac{1}{T} \int_0^T e^{i \arg[W_{s_1}(s, t) W_{s_2}^*(s, t)]} dt \right| \quad (4)$$

where  $T$  is the duration of the signal. This equation reflects the extent to which  $\phi_{1k,n}$  and  $\phi_{2k,n}$  (including the underlying activities) of both signals at each time  $t_n$  and frequency  $f$  are entirely correlated. Their relative phase difference is thus calculated as

$$\Delta\phi_{kn} = \phi_{2k,n} - \phi_{1k,n} \quad (5)$$

The phase coherence function  $C_\phi(f_k)$  is obtained by calculating and averaging in time the components of the sine and cosine of the phase differences for the whole signal, effectively defining the time-averaged WPC as

$$C_\phi(f_k) = \sqrt{\langle \cos\Delta\phi_{kn} \rangle^2 + \langle \sin\Delta\phi_{kn} \rangle^2} \quad (6)$$

The idea behind Equation (4) is that, while we are considering individual times and frequencies, these come from a discrete set (since all the signals in the present study are discrete and finite-time), and so the subscripts  $k$  and  $n$  just reflect this discreteness. The phase coherence function  $C_\phi(f_k)$  as defined in Equation (6) is exactly the discrete version of the phase coherence formula Equation (4), where  $\phi$  is the phase difference between the signals in question.

The tendency of  $\Delta\phi_{k,n}$  to remain constant, or not, at a certain frequency is characterized by the function  $C_\phi(f_k)$ , whose value lies between 0 and 1. The existence of phase coherence or incoherence is defined by  $C_\phi(f_k) \simeq 1$  or  $C_\phi(f_k) \simeq 0$  respectively. In the latter case  $C_\phi(f_k)$  varies continuously in time, whereas it remains unchanged (or stays within a small range) in the former.

Even in the case of two noisy signals, there is a tendency for there to be some apparent coherence in the sense that  $C_\phi(f_k)$  rarely approaches 0 at very low frequencies. The degree of apparent phase coherence depends on frequency. So the coherence baseline will not be the same for all scales. The low-frequency components, particularly signals of finite length (like ours) are evaluated using fewer periods than for the higher frequency components [30]. The result can be an

artificially increased coherence  $\approx 1$  even where, in reality, the dynamics of the signals are completely unrelated.

To remove this systematic bias toward low frequency components, a surrogate analysis test [66, 67] was employed, which creates a realization of the same system with no significant coherence. This is achieved by setting a null hypothesis that, for all frequencies, the phases  $\phi_{1\ k\ n}$  and  $\phi_{2\ k\ n}$  in the signals are independent. It is often referred to as the randomization of phase over time. A set of 100 amplitude-adjusted Fourier transform surrogates were generated by randomizing the phases of the reference signal, so as to create a new signal mimicking the reference signal, but without having any phase relationship to it. The significant wavelet phase coherence of the original signal was then obtained by subtracting from it the 95th percentile of the surrogate coherence.

### 2.3.3 | Statistical analysis

Because the BA and CA groups are unmatched, possible differences between them were tested using an unpaired two-sided Wilcoxon rank sum test, setting  $P < .05$  as the criterion for statistical significance. This method helps to check whether or not two groups of data emanate from the same distribution.

## 3 | RESULTS

Table 1 presents the anthropometric data. There are no significant age differences between the groups, and nor

are there any significant differences evident in their BMI, heart rate or diastolic or systolic blood pressures.

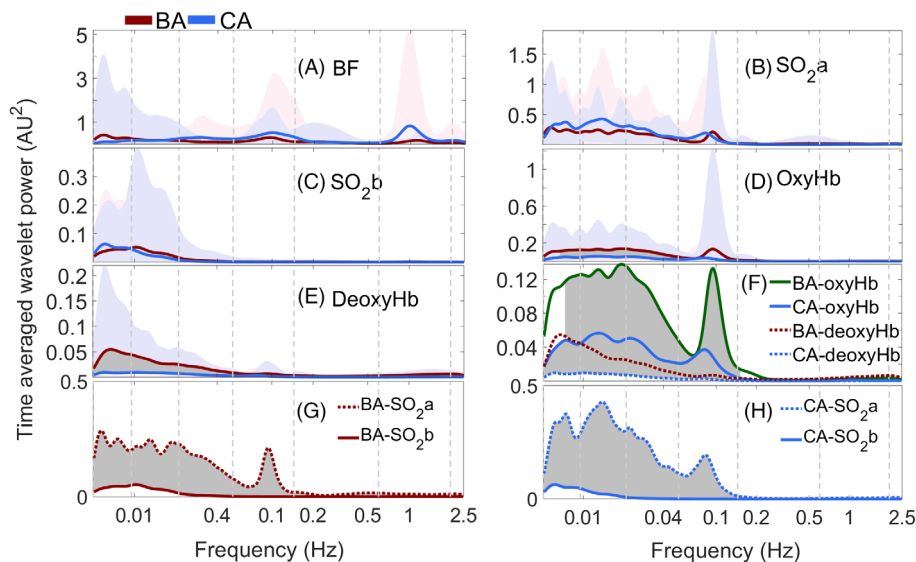
### 3.1 | Race-specific differences in skin perfusion, oxygen saturation and hemoglobin concentrations

Table 3 summarizes the results obtained for average microvascular blood flow, oxygen saturation and oxygenated and deoxygenated hemoglobin values, for each of the two groups. The mean oxygen saturations monitored using white light spectroscopy and NIRS were significantly lower ( $P = .002$  and  $P = .03$ , respectively) in BA than in CA. In contrast, the mean oxygenated and deoxygenated hemoglobin concentrations measured by white light spectroscopy were significantly higher in BA compared with CA ( $P = .002$  and  $P = .000001$ , respectively). There were no significant differences in skin perfusion as measured by LDF.

### 3.2 | Race-specific differences in spectral power

#### 3.2.1 | Microvascular blood flow

As indicated in Figure 1, the blood flow (BF) spectrum contains clearly resolved oscillatory components spanning the frequency range 0.0095 to 2 Hz. Intragroup comparison of the BF oscillations did not differ significantly in any of the six frequency intervals, as shown in



**FIGURE 2** Time-averaged wavelet power spectra of (A) blood flow (BF), (B-E) oxygenation parameters mean over groups. The comparison of the curves presented in (D,E) are summarized in (F). Lavender-blush and lavender shadings indicate the ranges between 5th and 95th percentiles in the BA and CA groups respectively, and gray shading in (D-H) indicates statistically significant ( $P < .05$ ) differences between the two groups. (G,H) Comparison between the oxygenation depths for the BA and CA groups respectively. Note that both  $SO_{2a}$  and  $SO_{2b}$  are expressed as %. The vertical lines indicate the six cardiovascular frequency intervals [55] within the range 0.0095 to 2 Hz

Figure 2A. The high peak in the cardiac interval of CA (Figure 2A) results from two outliers (subjects with very high cardiac peaks).

### 3.2.2 | Hemoglobin and oxygen saturation

Figure 1 also shows the typical time-averaged wavelet spectral power of oxygen saturation  $SO_{2a}$  (obtained using white light spectroscopy), oxygen saturation  $SO_{2b}$  (obtained using NIRS), oxygenated hemoglobin (oxyHb) and deoxygenated hemoglobin (deoxyHb), recorded from a black African and a Caucasian. Unlike the case of BF, high frequency peaks are not clearly resolved in  $SO_{2a}$ ,  $SO_{2b}$  and oxyHb power spectra, as they appeared noisy, but their low frequency spectral content could be clearly visualized in both the BA and CA subjects, as shown in Figure 2. In contrast, neither the low nor high frequency components were clearly observed in the deoxyHb spectrum.  $SO_{2a}$  and  $SO_{2b}$  recorded from the skin and deeper tissue exhibit similar power spectra ( $P > .05$ ) across the 0.0095 to 2 Hz frequency interval, when compared between BA and CA groups, while their spectral powers at frequency  $> 0.1$  Hz are diminished in both cases, as shown in Figure 2B,C. In contrast to  $SO_{2a}$  and  $SO_{2b}$ , the power, oxyHb and deoxyHb spectral power were significantly higher in BA compared with CA ( $P > .05$ ) groups in the frequency intervals IV, V and VI associated with neurogenic, NO dependent endothelial and NO independent endothelial activity (Figure 2D,E). No significant difference was observed in either the oxyHb or deoxyHb spectral powers ( $P > .05$ ) between groups above

0.4 Hz, partly because the power diminishes within the high frequency intervals. The intra-group comparison of oxyHb and deoxyHb spectral powers (within each group) showed a marked difference between the hemoglobin concentrations (power) in BA and CA groups (Figure 2F).

### 3.3 | Race-specific differences in wavelet phase coherence

#### 3.3.1 | Coherence between fluctuations in blood flow and oxygen saturation

Figure 3 presents the wavelet phase coherences between oscillations in BF and  $SO_{2a}$ , BF and  $SO_{2b}$ . The CA group showed significantly higher phase coherence between BF and  $SO_{2a}$  in the frequency intervals associated with cardiac (I) and myogenic (III) activity ( $P = .0075$  and  $P = .0003$ , respectively) compared to BA. The coherence nearly disappears in the respiratory frequency interval in both groups. In contrast, a comparison between BA and CA reveals no significant coherence between BF and  $SO_{2b}$  (Figure 3) across the 0.0095 to 2 Hz frequency interval, nor in the cardiac and myogenic frequency band, although the former and latter were slightly seen to be lower, but not significantly.

#### 3.3.2 | Coherence between fluctuations in blood flow and hemoglobin

Wavelet phase coherence between oscillations in BF and both oxyHb and deoxyHb were calculated and the group

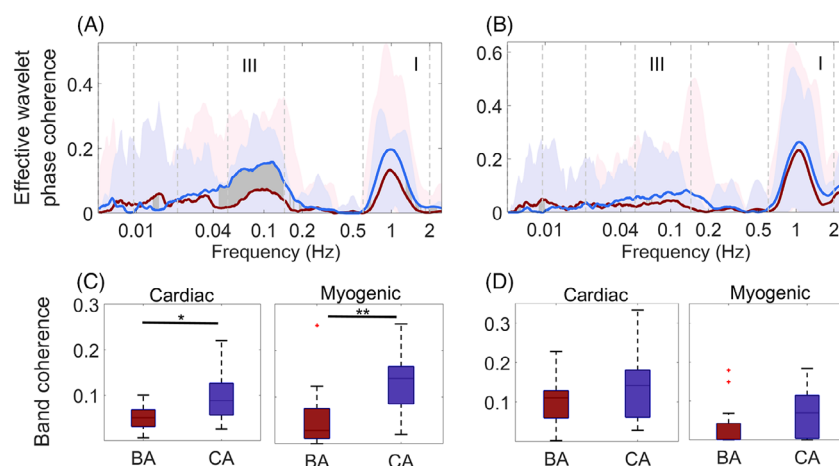


**FIGURE 3** Blood flow and oxygen saturation phase coherence, and means over groups. Wavelet phase coherence (minus surrogate thresholds) between (A) BF and  $SO_{2a}$  (oxygen saturation recorded using white light spectroscopy). (B) BF and  $SO_{2b}$  (oxygen saturation recorded using NIRS), where III and I indicate the myogenic and cardiac frequency intervals respectively. Lavender-blush and lavender shadings indicate the ranges between 5th and 95th percentiles in the BA and CA groups respectively, and gray shading indicates statistically significant ( $P < 0.05$ ) differences between BA and CA. The box-plots show the coherence between (C) BF and  $SO_{2a}$ , and (D) BF and  $SO_{2b}$  within the cardiac and myogenic frequency intervals. \* $P < .05$ , \*\* $P < 0.005$



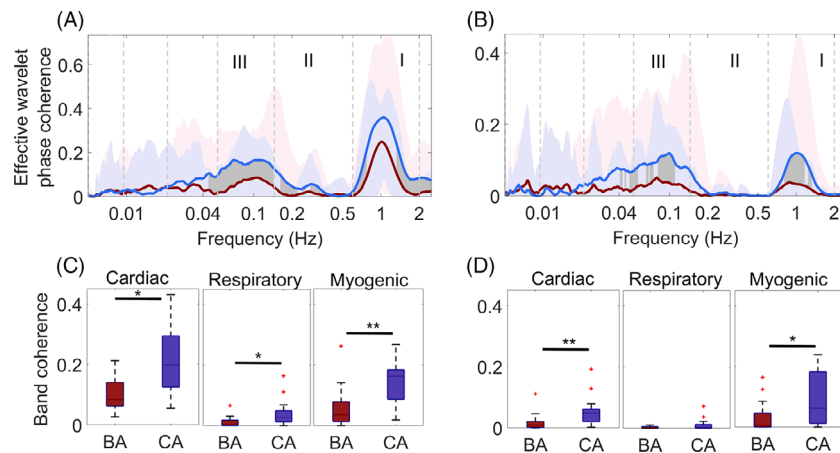
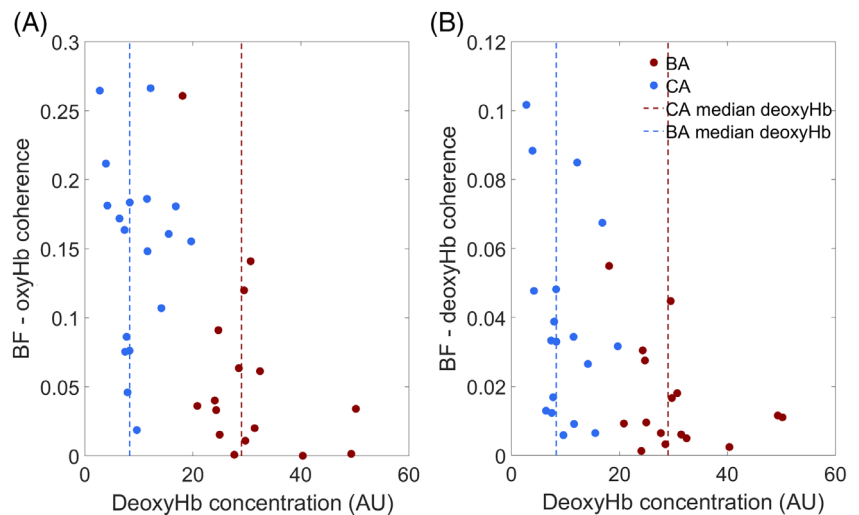


**FIGURE 4** Blood flow and hemoglobin phase coherence, and means over groups. Wavelet phase coherence (minus surrogate thresholds) between (A) BF and oxyHb (B) BF and deoxyHb, where III, II and I indicates myogenic, respiratory, cardiac frequency intervals respectively. Lavender-blush and lavender shadings indicate the ranges between 5th and 95th percentiles in the BA and CA groups respectively, and gray shading indicates statistically significant ( $P < .05$ ) differences between BA and CA. The box-plots show coherence between (C) BF and oxyHb, and (D) BF and deoxyHb within the cardiac, respiratory, and myogenic frequency ranges. \* $P < .05$ , \*\* $P < .005$

**FIGURE 5** Relationship between the deoxygenated hemoglobin concentration and the estimated wavelet phase coherences between blood flow and oxygenated/deoxygenated signals. (A) Coherence between blood flow and oxygenated hemoglobin plotted against the deoxyHb signal, (B) Coherence between blood flow and deoxygenated hemoglobin plotted against the deoxyHb concentration



mean coherence is shown in Figure 4A,B. A significantly higher coherence between BF and oxyHb was observed in CA in the frequency intervals I, II and III ( $P = .0061$ ,  $P = .005$ ,  $P = .0004$ , respectively) associated with cardiac, respiratory and myogenic activity, respectively (Figure 4). In the coherence between BF and deoxyHb, CA exhibited a significantly higher coherence in only the cardiac and myogenic frequency intervals ( $P = .001$  and  $P = .01$ , respectively), while no such significant difference ( $P = .13$ ) was observed in the respiratory interval, as the coherence in the latter interval was diminished in both groups. BA exhibited a significantly lower phase coherence in all frequency intervals where significant differences were observed, as presented in Figure 4C,D.

### 3.3.3 | Linear relation between blood flow - hemoglobin coherence and deoxyHb concentration

Figure 5 presents linear graphs expressing the relationships between the estimated BF and oxyHb/deoxyHb coherence and deoxyHb concentration. As deoxyHb increases in BA, the coherence between BF and oxyHb decreases, while the low deoxyHb concentration in CA leads in turn to high coherence between BF and oxyHb (Figure 5). In a similar fashion, the higher deoxyHb concentration in CA reduces the coherence between BF and deoxyHb, while the reverse is the case for BA (Figure 5B).

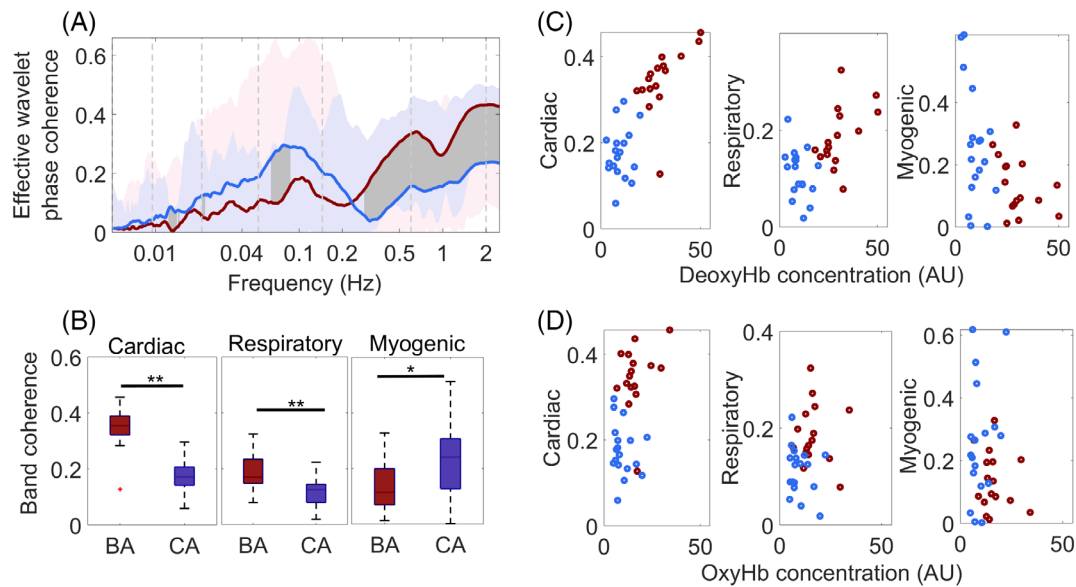


**FIGURE 6** Phase coherence between hemoglobin signals and its comparison with the oxygenated/deoxygenated hemoglobin concentrations: (A) Wavelet phase coherence (minus surrogate thresholds) between oxyHb and deoxyHb concentrations, mean over groups. Lavender-blush and lavender shadings indicate the ranges between 5th and 95th percentiles in the BA and CA groups respectively, and gray shading indicates statistically significant ( $P < 0.05$ ) differences between BA and CA. (B) Box-plots showing coherence between the oxyHb and deoxyHb signals in the cardiac, respiration and myogenic frequency ranges. Comparisons of cardiac, respiratory and myogenic oscillatory activities in oxyHb—deoxyHb coherence with (C) deoxyHb and (D) oxyHb concentrations. \* $P < .05$ , \*\* $P < .005$

### 3.3.4 | Coherence between oxygenated and deoxygenated hemoglobin concentrations

Analysis of phase coherence between oxygenated and deoxygenated hemoglobin are summarized in Figure 6. A significantly lower phase coherence in the frequency intervals associated with cardiac, respiratory and myogenic activity ( $P = .00001$ ,  $P = .0004$  and  $P = .04$ , respectively) was observed in the CA group as compared to BA (Figure 6). Although not statistically significant, CA exhibited a slightly higher coherence below 0.052 Hz with the coherence nearly disappearing toward 0.0095 Hz (Figure 6).

### 3.3.5 | Linear relation between oxygenated and deoxygenated hemoglobin coherence and hemoglobin concentration

Figures 6C,D present linear graphs illustrating the relationships between the estimated oxyHb and deoxyHb wavelet phase coherence and level of hemoglobin (oxyHb and deoxyHb) concentration, in the frequency intervals associated with cardiac, respiratory and myogenic activity. As the deoxyHb concentration is higher in BA, the phase coherence between oxyHb and deoxyHb in cardiac frequency band is correspondingly higher. In contrast, low deoxyHb in CA leads to low coherence between oxyHb and deoxyHb in the

cardiac frequency interval. Unlike the cardiac band coherence, no marked relationship between deoxyHb level and coherence in either the respiratory or myogenic frequency band was observed (Figure 6C).

Figure 6D illustrates that, under almost the same level of oxyHb in BA and CA, the coherence between oxyHb and deoxyHb is higher in the cardiac frequency band of BA than in that of CA. No such relationship is observed in the other frequency bands.

## 4 | DISCUSSION

By analysis of phase coherence between the oscillations in microvascular blood flow and tissue oxygenation we have been able to study how cardiovascular and microvascular dynamical processes differ between black Africans and Caucasians, using only resting-state recordings obtained from combined LDF and white light spectroscopy.

A study of sepia melanin spectra has shown that melanin generally exhibits high absorption in the UV region at 200 to 300 nm, but that the absorption diminishes toward the visible region [68]. Further reports [69–71] confirm that the typical absorption spectrum of melanin exhibits high absorption in the UV to visible spectral range, with an almost featureless spectrum, and that there is a monotonic decrease in absorption when moving from the UV through the visible to NIR spectral region.

Moreover, a model of fluorescence spectra from biological tissue based on the Monte Carlo approach has predicted the effect of melanin concentration on a spectroscopy signal [72]. The use of near-IR diode lasers of relatively long wavelength (670, 780 and 810 to 850 nm) was shown to improve optical penetration [73]. In addition, Fredriksson et al. [74] used Monte Carlo simulations of light propagation in tissue, for wavelengths between 543 and 780 nm, to show that skin pigmentation is expected to have a negligible effect on the measurement depth. Although it is clear that the wavelength of the light influences optical penetration, irrespective of skin color, our discussion of differences in oxy- and deoxyhemoglobin between the groups should be treated with a degree of caution because some of the difference could be on account of the different melanin concentrations. However, no such caveat is needed in relation to the dynamics which provides our main focus of interest.

The significantly higher concentrations of both oxygenated and deoxygenated hemoglobin in the BA group may be related to the effect of high altitude on hemoglobin concentrations [75]: the BA subjects have lived at altitudes above 500 m for most of their lives, unlike the members of the CA group who have lived mostly at up to 50 m above sea level. It is known that the hemoglobin concentration present in the blood of those who live at high altitude is greater, helping to compensate for the lower partial pressure of oxygen in the atmosphere.

The median values of  $SO_2a$  and  $SO_2b$  are different within each of the groups as shown in Table 3, and differ significantly between the groups. The difference within each group can be attributed to the differing depths of measurement. Whereas the oxygen saturation level obtained with white light spectroscopy reflects oxygen saturation measured in superficial skin, that obtained with NIRS reflects the levels in deeper skin.

Wavelet analyses of the microvascular blood flow and oxygenation time-series revealed the major oscillatory activities that manifest in these signals (see Figures 1 and 2). Cardiac (0.6-2.0 Hz), respiratory (0.15-0.6 Hz) and lower frequency components (below 0.15 Hz) are visible in both types of signal, though at different strengths.  $SO_2b$  signals exhibit stronger low frequency components, because they relate to metabolic processes. In terms of power, however, the BF signal has a stronger cardiac component because, even in the microvasculature, the blood flow is still pulsatile. The higher power in the lower-frequency intervals of other signal indicates that the movements of  $O_2$ ,  $SO_2$  and Hb are modulated mainly by cell and tissue-perfusion-related oscillatory processes.

The significant difference between the BA and CA groups in oxygenated and deoxygenated hemoglobin spectral power in the very low frequency (<0.05 Hz)

oscillatory intervals may indicate a higher NO level in BA. The increased NO may serve as a way of boosting oxygen uptake following the effect of high altitude on hemoglobin concentration. Oscillations in the 0.021 to 0.052 Hz frequency intervals are mediated by vasomotion in small arterioles, reflecting the neurogenic response, and have been observed previously in oxygenation dynamics [28, 29]. The higher neurogenic spectral power might therefore imply that arterioles are more dilated in BA. It has been suggested that, apart from relaxing the blood vessels, NO may also increase the release of oxygen from hemoglobin [76]. Associated with the higher hemoglobin concentration in BA, one might expect higher NO production. These effects might account for the higher spectral power associated with the neurogenic and endothelial activity in the BA group.

Following a meta-analysis [35] suggesting that race-specific differences can have a significant effect on  $HbA_{1c}$  levels, Richard et al. in their experimental study recently identified a higher mean  $HbA_{1c}$  level in black subjects than in whites. The reason is not yet understood, but a potentially fruitful approach is to study oxygenation parameters alongside their dynamical variations on a continuous time scale, without need for the subjects to be glycated, as in the present article.

Our findings on the differences in hemoglobin concentrations were similar to the differences observed between blacks and whites in the  $HbA_{1c}$  study. The significantly higher oxyHb and deoxyHb concentrations in BA (Table 3) are consistent with the mean  $HbA_{1c}$  levels being higher in blacks than in whites, as reported in several earlier studies [33]. However, the reverse was the case for mean oxygen saturation measured with white light spectroscopy, and NIRS, as the average oxygen saturations were significantly lower in the BA group. Blood perfusion recordings did not differ between groups. We assumed that the volume of blood flowing through the microvasculature is not influenced by race-specific differences, even where the hemoglobin concentration is different.

The low oxygen saturation exhibited by BA group (Table 3) could perhaps be related to plasma skimming—considering that, at higher altitude, atmospheric oxygen levels are lower, leading to increased erythrocyte density and hematocrit to enable more oxygen to be delivered to the tissues. An investigation of microvascular hematocrit and its possible relation to oxygen supply indicated that processes such as muscle contraction and vasodilation (which are known to manifest in microvascular dynamics) could potentially influence the *in vivo* capillary hematocrit [77, 78]. The dynamic coordination between plasma skimming and the effect of blood viscosity on hematocrit can produce spontaneous oscillations in

capillary blood flow (skin microcirculation) [78]. Further investigation of such coordination and its effect on oscillations in blood flow and oxygenation would be very interesting.

Oscillations in blood flow and oxygen saturation across the full frequency interval 0.0095 to 2 Hz were not influenced by race, in the sense that their power spectra did not differ significantly between the two groups. However, oscillations in oxyHb and deoxyHb measured with white light spectroscopy exhibited significant race-specific differences. Higher spectral power in the oxyHb and deoxyHb of the BA group was found in the very low frequency interval. This may imply that hemoglobin in the BA group has a low affinity for oxygen, causing oxygen to bind swiftly to the heme component of the hemoglobin in the red blood cells during respiration. In a similar manner, oxygen may get released rapidly from the hemoglobin.

The lower phase coherence between oscillations in microvascular blood flow and skin oxygen saturation in the cardiac and myogenic interval for the BA group (Figure 3A) indicates an additional race-specific difference in the cardiovascular system. In similar fashion, the phase coherence in cardiac and myogenic intervals of the blood flow and oxygenation at deeper tissue were slightly smaller in BA, although not significantly (Figure 3D). The results seem to imply a progressive alteration or compromise that gene expression may impose on the underlying mechanism of coordination between the microcirculation and the balance between oxygen delivery/demand, with consequences for the vasculature.

Similarly, phase coherence in the cardiac, respiratory and myogenic oscillations in blood flow and oxygenated/deoxygenated hemoglobin were significantly lower in BA, together with lower coherence between respiratory oscillations in blood flow and oxygenated hemoglobin (Figure 4). The results further confirm our findings in relation to coherence between blood flow and oxygen saturation, and could be related to an attenuation in the cardiac and myogenic oscillations of the vascular smooth wall [79], particularly during the mutual interaction between processes of blood flow and hemoglobin dynamics. The lower coherence (Figures 3A,D and Figures 4A,B) in the myogenic frequency band of the BA group could possibly be associated with the higher average temperature in Sub-Saharan Africa compared to Europe: the average temperature is what determines the average degree of vasodilation [80, 81], which will differ between Africans (living mostly at temperatures above 20°C) and Europeans (living mostly below 20°C).

Note that the model (modified Beer-Lambert law) used in calculating oxygenation and hemoglobin concentration is premised on an assumption that deserves

comment. First, the model accounts for attenuation by summing the mean path length of detected photons, which is argued by Sassaroli and Fantini [82] to be incorrect. They proved the need for averaging the mean path length of detected photons over the range of absorption coefficient and not just simply considering the sum. Nonetheless the authors still agree that even the supposed imperfect form of the model accurately evaluates the variability in the absorption coefficient of the medium. The changes in its absorption coefficient are related to the variability in the optical signal. Second, we would comment that the analysis of skin parameters where there is high melanin concentration remains a challenging task, although it has been addressed through hyperspectral imaging of the skin [83]. Due to the high statistically decreased levels of oxygenation, however, it is unlikely that these differences emanate from the attenuated signal level or from the presence of artifacts when fitting the measured spectrum signal with the model of the reflectance spectroscopy.

The marked attenuation in coherence between blood flow and skin oxygenation in the cardiac and myogenic intervals for the BA group compared to CA may have been associated with the highly deoxygenated hemoglobin concentration level present in BA, an inference that is supported by an additional finding: higher deoxygenated hemoglobin concentration is associated with significant reduction in the coherences between blood flow and oxygenated/deoxygenated hemoglobin (Figure 5). This may perhaps relate to the altered cardiac and myogenic activity observed via the coherence between oxygenated and deoxygenated hemoglobin signals (Figure 6). The coherences between  $SO_2a$  and  $SO_2b$  did not differ significantly between the BA and CA groups, and therefore are not shown. The implication is that no coherence exists between shallow depth and deeper skin layers containing larger vessels and skeletal muscle respectively. The oxygenation dynamics (power) differs markedly between the two layers, particularly in the low frequency intervals Figures 2G,H. Oscillations around the respiratory frequency interval mainly contribute to the spectral power of oxygenation measured at the deeper skin depth, while the low frequency components mainly contribute to the power measured at shallow skin depths. Our findings are consistent with a previous study conducted on light-skinned participants with low melanin concentrations, which suggested a difference in the pattern of blood flow and oxygenation dynamics between these layers [30]. Note that in the present study the two oxygenation signals are measured by different methods; by scaling and displaying as %, however, they can be directly compared.

The degree of coordination between oscillatory activity in the LDF, white light spectroscopy and NIRS signals can be evaluated by wavelet-based phase coherence analysis. In the BA group, intervals of significantly higher wavelet phase coherence between blood flow and oxyHb were found at 0.05 to 0.3 Hz, and to some extent within 0.5 to 2 Hz; but this was only partly so for coherence between blood flow and deoxyHb. This evidence explains the hemoglobin spectral power results, that is, in the BA group the hemoglobin has low affinity for oxygen. This follows from the rapid release of oxygen from the heme protein hemoglobin, resulting in a high coherence in the 0.05 to 0.3 Hz and 0.5 to 2 Hz intervals. Note that the observed differences in the BFOD of the BA and CA groups do not result from the effects of differing light penetration in skin with different melanin concentration because, for illumination at wavelengths >750 nm, LDF is unaffected by skin pigmentation [54].

We emphasize the particular advantage of wavelet phase coherence analysis in the present context. In earlier approaches, frequency-domain analyses were used to seek relationships between signals by detecting frequency ranges that shared ranges of relatively high/low power; in addition, the WT was used to explore these ranges in the time-frequency domain [19, 84]. The fact of sharing high/low power at a particular frequency and time does not, however, necessarily signify a common cause. A better indicator of either mutual interaction or common influence between two signals, is the existence of a common phase relationship between oscillatory components. This can conveniently be evaluated through their degree of wavelet phase coherence [17], which remains valid even in the case of time-varying frequency and is robust in the face of noise and perturbations. Here, the use of combined optical methods has provided for the simultaneous evaluation of microvascular blood flow and skin oxygenation at closely adjacent points. It has allowed analyses of rhythmic coordination, illuminating how oxygen is consumed within the capillary bed and, based on wavelet phase coherence between LDF and white light spectroscopy signals, has confirmed some known race-specific differences and revealed other differences that were hitherto unknown.

## 5 | CONCLUSIONS

By investigating the deterministic properties of simultaneously recorded microvascular blood flow and skin oxygenation signals, using combined optical LDF and white light spectroscopy and oxygenation measured at a deeper level in the tissue with near infrared spectrometer, and by extracting time-varying oscillatory parameters and phase coherences, we have gained new insights into race-related

differences in microvascular dynamics. While coherence between fluctuations in blood flow and oxygenation in general have been studied previously, here we have investigated for the first time race-specific differences in phase coherence between blood flow and oxygenation oscillations within the 0.0095 to 2 Hz frequency interval. The significant alteration of coherence within the cardiac, myogenic and respiratory intervals of the BA group as captured in the microvasculature seems to imply that some of the underlying physiological mechanisms manifest in the cardiovascular dynamics function in a slightly different way. This suggests small differences of microvascular regulation between the BA and CA groups. Similarly, the BA subjects differ from Caucasians of the same age in the spectral powers of their oxygenated and deoxygenated hemoglobin in the neurogenic and endothelial oscillations—both NO dependent and independent—within the microvascular network. Thus race-specific differences affect the local and systemic components of the cardiovascular system by attenuating rhythmic coordination between the oscillators of which it is composed. Although the physiological meanings of these findings are yet to be fully evaluated, our approach provides robust insight into race-related differences of coherence in cardiovascular pathophysiology.

## ACKNOWLEDGMENTS

We are grateful to the participants who generously volunteered to be measured in this project and to Rodney Gush and Brian Lock of Moor Instruments Ltd, Axminster, UK, for providing useful support and the equipment used for the experiments.

## CONFLICT OF INTEREST

The authors declare no potential conflict of interests.

## AUTHOR CONTRIBUTIONS

Y.A.A. carried out the measurements and analysis and drafted the text; P.V.E.McC. helped with the text; A.S. coordinated the project. All authors participated in the planning of the project and edited the text.

## ORCID

Aneta Stefanovska  <https://orcid.org/0000-0001-6952-8370>

## REFERENCES

- [1] A. L. Hinderliter, A. R. Sager, A. Sherwood, K. C. Light, S. S. Girdler, P. W. Willis, *Am. J. Cardiol.* **1996**, *78*(2), 208.
- [2] E. M. Urbina, W. Bao, A. S. Pickoff, G. S. Berenson, *Am. J. Hypertens.* **1998**, *11*(2), 196.
- [3] X. Wang, *Am. J. Cardiol.* **2005**, *96*(8), 1166.
- [4] L. C. Peng Wei, J. Milbauer, J. Enenstein, W. Nguyen, R. P. H. Pan, *BMC Med.* **2011**, *9*(1), 2.

- [5] C. M. Carmine Cardillo, R. O. Kilcoyne, I. I. I. Cannon, J. A. Panza, *Hypertension* **1998**, *31*(6), 1235.
- [6] C. M. Carmine Cardillo, R. O. Kilcoyne, I. I. I. Cannon, J. A. Panza, *Circulation* **1999**, *99*(1), 90.
- [7] I. T. Leszek Kalinowski, T. M. Dobrucki, *Circulation* **2004**, *109* (21), 2511.
- [8] M. A. Ozkor, A. M. Rahman, J. R. Murrow, N. Kavtaradze, J. Lin, A. Manatunga, S. Hayek, A. A. Quyyumi, *Arterioscler. Thromb. Vasc. Biol.* **2014**, *34*, 1320.
- [9] K. Kim, C. Hurr, C. Jordan, R. M. B. Patik, *Microvasc. Res.* **2018**, *118*, 1.
- [10] D. F. Dluzen, N. N. Hooten, Y. Zhang, Y. Kim, F. E. Glover, S. M. Tajuddin, K. D. Jacob, A. B. Zonderman, M. K. Evans, *Sci. Rep.* **2016**, *6*, 35815.
- [11] H. D. Kvernmo, A. Stefanovska, K. A. Kirkeboen, K. Kvernebo, *Microvasc. Res.* **1999**, *57*(3), 298.
- [12] A. Koller, G. Kaley, *Am. J. Physiol. Heart Circ. Physiol.* **1991**, *260*(3), H862.
- [13] R. E. Michael, M. S. Olson, H. N. Williford, *J. Appl. Res.* **2010**, *10*(1), 24.
- [14] M. Heideman, D. Johnson, C. Burrus, *IEEE ASSP Mag* **1984**, *1* (4), 14.
- [15] P. Clemson, A. Stefanovska, *Phys. Rep.* **2014**, *542*(4), 297.
- [16] J.-P. Lachaux, A. Lutz, D. Rudrauf, D. Cosmelli, M. Le Van Quyen, J. Martinerie, F. Varela, *Neurophysiol. Clin.* **2002**, *32* (3), 157.
- [17] A. Bandrivskyy, A. Bernjak, P. McClintock, A. Stefanovska, *Cardiovasc. Eng.* **2004**, *4*(1), 89.
- [18] L. W. Sheppard, A. Stefanovska, P. V. E. McClintock, *Phys. Rev. E* **2012**, *85*, 046205.
- [19] A. Stefanovska, M. Bracic, H. D. Kvernmo, *IEEE Trans. Biomed. Eng.* **1999**, *46*(10), 1230.
- [20] T. Söderström, A. Stefanovska, M. Veber, H. Svensson, *Am. J. Physiol. Heart Circ. Physiol.* **2003**, *284*(5), H1638.
- [21] S. Bertuglia, A. Colantuoni, G. Coppini, M. Intaglietta, *Am. J. Physiol. Heart Circ. Physiol.* **1991**, *260*(2), H362.
- [22] R. D. Braun, J. L. Lanzen, M. W. Dewhirst, *Am. J. Physiol. Heart Circ. Physiol.* **1999**, *277*(2), H551.
- [23] C. E. Thorn, A. C. Shore, S. J. Matcher, *Optical Tomography and Spectroscopy of Tissue VII*. in *International Society for Optics and Photonics*. SPIE conference proceedings, Bellingham, Washington, **2007**, 643421.
- [24] A. Stefanovska, *Am. J. Physiol. Heart Circ. Physiol.* **2009**, *296* (5), H1224.
- [25] A. Krogh, *J. Physiol.* **1919**, *52*(6), 391.
- [26] A. Krogh, *J. Physiol.* **1919**, *52*(6), 409.
- [27] D. S. Vikram, J. L. Zweier, P. Kuppusamy, *Antioxid. Redox Signal.* **2007**, *9*(10), 1745.
- [28] C. E. Thorn, S. J. Matcher, I. V. Meglinski, A. C. Shore, *Am. J. Physiol. Heart Circ. Physiol.* **2009**, *296*(5), H1289.
- [29] C. E. Thorn, H. Kyte, D. W. Slaff, A. C. Shore, *Am. J. Physiol. Heart Circ. Physiol.* **2011**, *301*(2), H442.
- [30] A. Bernjak, A. Stefanovska, P. V. E. McClintock, P. J. Owen-Lynch, P. B. M. Clarkson, *Fluct. Noise. Lett.* **2012**, *11*(1), 1240013.
- [31] T. Yano, C.-S. Lian, R. Afroundeh, K. Shirakawa, T. Yunoki, *Biol. Sport* **2014**, *31*(1), 15.
- [32] R. M. Cohen, H. Snieder, C. J. Lindsell, H. Beyan, M. I. Hawa, S. Blinko, R. Edwards, T. D. Spector, D. G. Leslie, *Diabetes Care* **2006**, *29*(8), 1739.
- [33] R. M. Bergenstal, R. L. Gal, C. G. Connor, R. Gubitosi-Klug, D. Kruger, B. A. Olson, S. M. Willi, G. Aleppo, R. S. Weinstock, J. Wood, M. Rickels, *Ann. Intern. Med.* **2017**, *167*(2), 95.
- [34] J. M. Boltri, I. S. Okosun, M. Davis-Smith, R. L. Vogel, *Ethn. Dis.* **2005**, *15*(4), 562.
- [35] J. K. Kirk, R. B. D'Agostino, R. A. Bell, L. V. Passmore, D. E. Bonds, A. J. Karter, K. M. V. Narayan, *Diabetes care* **2006**, *29*(9), 2130.
- [36] D. C. Ziemer, P. Kolm, W. S. Weintraub, V. Vaccarino, M. K. Rhee, J. G. Twombly, K. M. V. Narayan, D. D. Koch, L. S. Phillips, *Ann. Intern. Med.* **2010**, *152*(12), 770.
- [37] E. Selvin, M. W. Steffes, C. M. Ballantyne, R. C. Hoogeveen, J. Coresh, F. L. Brancati, *Ann. Intern. Med.* **2011**, *154*(5), 303.
- [38] W. H. Herman, R. M. Cohen, *J. Clin. Endocrinol. Metab.* **2012**, *97*(4), 1067.
- [39] W. H. Herman, *Diabetes Care* **2016**, *39*(8), 1458.
- [40] E. Selvin, *Diabetes Care* **2016**, *39*(8), 1462.
- [41] F. F. Jobsis, *Science* **1977**, *198*(4323), 1264.
- [42] Mark Cope, *Ph.D. Thesis*, University of London, **1991**.
- [43] M. Thanaj, A. J. Chipperfield, G. F. Clough, *Comput. Biol. Med.* **2018**, *102*, 157.
- [44] M. Thanaj, A. J. Chipperfield, G. F. Clough, *World Congress on Medical Physics and Biomedical Engineering 2018*, Springer, New York, NY, **2019**, p. 195.
- [45] M. D. Stern, *Appl. Opt.* **1985**, *24*(13), 1968.
- [46] V. Dremin, I. Kozlov, M. Volkov, N. Margaryants, A. Potemkin, E. Zhrebtsov, A. Dunaev, I. Gurov, *J. Biophotonics* **2019**, *12*(6), e201800317.
- [47] A. G. Tsai, M. Intaglietta, *Int. J. Microcirc. Clin. Exp.* **1993**, *12* (1), 75.
- [48] D. Goldman, A. S. Popel, *J. Theor. Biol.* **2001**, *209*(2), 189.
- [49] M. A. Franceschini, D. A. Boas, A. Zourabian, S. G. Diamond, S. Nadgir, D. W. Lin, J. B. Moore, S. Fantini, *J. Appl. Physiol.* **2002**, *92*(1), 372.
- [50] Z. Li, Y. Wang, Y. Li, Y. Wang, J. Li, L. Zhang, *Microvasc. Res.* **2010**, *80*(1), 142.
- [51] V. V. Kislukhin, *Math. Biosci.* **2004**, *191*(1), 101.
- [52] T.-L. Wang, C.-R. Hung, *Ann. Emerg. Med.* **2004**, *44*(3), 222.
- [53] F. C. Ramirez, S. Padda, S. Medlin, H. Tarbell, F. W. Leung, *Am. J. Gastroenterol.* **2002**, *97*(11), 2780.
- [54] Y. A. Abdulhameed, G. Lancaster, P. V. E. McClintock, A. Stefanovska, *Physiol. Meas* **2019**, *074005*, 40.
- [55] Y. Shiogai, A. Stefanovska, P. V. E. McClintock, *Phys. Rep.* **2010**, *488*(2–3), 51.
- [56] C. Aalkjær, D. Boedtker, V. Matchkov, *Acta. Physiol.* **2011**, *202*(3), 253.
- [57] S. J. Matcher, C. E. Elwell, C. E. Cooper, M. Cope, D. T. Delpy, *Anal. Biochem.* **1995**, *227*(1), 54.
- [58] S. Suzuki, S. Takasaki, T. Ozaki, Y. Kobayashi, *Optical Tomography and Spectroscopy of Tissue III*, International Society for Optics and Photonics, SPIE conference proceedings, Bellingham, Washington, **1999**, p. 582.
- [59] S. J. Matcher, P. J. Kirkpatrick, K. Nahid, M. Cope, D. T. Delpy, *Optical Tomography, Photon Migration, and Spectroscopy of Tissue and Model Media: Theory, Human Studies, and Instrumentation*. in *International Society for Optics and Photonics*, SPIE conference proceedings Bellingham, Washington, **1995**, 3597, p. 486.

- [60] Hongyuan Liu, M. Kohl-Bareis, X. Huang, *European Conference on Biomedical Optics*, Optical Society of America, Washington, DC, **2011**, 80871Y1-10.
- [61] F. Mormann, K. Lehnertz, P. David, C. E. Elger, *Physica D* **2000**, 144(3-4), 358.
- [62] A. Pikovsky, M. Rosenblum, J. Kurths, *Synchronization – A Universal Concept in Nonlinear Sciences*, Cambridge University Press, Cambridge **2001**.
- [63] A. E. Hramov, A. A. Koronovskii, V. I. Ponomarenko, M. D. Prokhorov, *Phys. Rev. E* **2007**, 75(5), 056207.
- [64] A. S. Karavaev, M. D. Prokhorov, V. I. Ponomarenko, A. R. Kiselev, V. I. Gridnev, E. I. Ruban, B. P. Bezruchko, *Chaos* **2009**, 19(3), 033112.
- [65] P. Clemson, G. Lancaster, A. Stefanovska, *Proc. IEEE* **2016**, 104(2), 223.
- [66] T. Schreiber, A. Schmitz, *Phys. Rev. Lett.* **1996**, 77(4), 635.
- [67] G. Lancaster, D. Iatsenko, A. Pidde, V. Ticcinelli, A. Stefanovska, *Phys. Rep.* **2018**, 748, 1.
- [68] A. Mbonyiryivuze, I. Omollo, B. D. Ngom, B. Mwakikunga, S. M. Dhlamini, E. Park, M. Maaza, *Sci. Educ.* **2015**, 3(1), 1.
- [69] M Magarelli, *Ph.D. Thesis*, Macerata: University of Camerino, **2011**.
- [70] Z. Huang, H. Lui, M. X. K. Chen, A. Alajlan, D. I. McLean, H. Zeng, *J. Biomed. Opt.* **2004**, 9(6), 1198.
- [71] G. Perna, M. Lasalvia, C. Gallo, G. Quartucci, V. Capozzi, *The Open Surf Sci J* **2013**, 5, 1-8.
- [72] V. V. Dremin, A. V. Dunaev, *J. Opt. Technol.* **2016**, 83, 43.
- [73] A. K. Murray, A. L. Herrick, T. A. King, *J. Rheumatol.* **2004**, 43, 1210.
- [74] I. Fredriksson, M. Larsson, T. Stromberg, *Microvasc. Res* **2009**, 78(1), 4.
- [75] T. Wu, X. Wang, C. Wei, H. Cheng, X. Wang, Y. Li, H. Zhao, P. Young, G. Li, Z. Wang, et al., *J. Appl. Physiol.* **2005**, 98(2), 598.
- [76] H. Kosaka, *Biochim. Biophys. Acta. Bioenerg.* **1999**, 1411(2), 370.
- [77] B. Klitzman, B. R. Duling, *Am. J. Physiol. Heart Circ. Physiol.* **1979**, 237(4), H481.
- [78] W. H. Reinhart, N. Z. Piety, S. S. Shevkoplyas, *Microcirculation* **2017**, 24(8), e12396.
- [79] K. Lossius, M. Eriksen, *Microvasc. Res.* **1995**, 50(1), 94.
- [80] L. W. Sheppard, V. Vuksanović, P. V. E. McClintock, A. Stefanovska, *Phys. Med. Biol.* **2011**, 56, 3583.
- [81] A. Bernjak, J. Cui, S. Iwase, T. Mano, A. Stefanovska, D. L. Eckberg, *J. Physiol* **2012**, 590(2), 363.
- [82] A. Sassaroli, S. Fantini, *Phys. Med. Biol.* **2004**, 49(14), N255.
- [83] E. Zherebtsov, V. Dremin, A. Popov, A. Doronin, D. Kurakina, M. Kirillin, I. Meglinski, A. Bykov, *Biomed. Opt. Express* **2019**, 10(7), 3545.
- [84] M. Bračić, A. Stefanovska, *Bull. Math. Biol.* **1998**, 60(5), 919.

**How to cite this article:** Abdulhameed YA, McClintock PVE, Stefanovska A. Race-specific differences in the phase coherence between blood flow and oxygenation: A simultaneous NIRS, white light spectroscopy and LDF study. *J. Biophotonics*. 2020;e201960131. <https://doi.org/10.1002/jbio.201960131>